Defence Science Journal, Vol. 66, No. 6, November 2016, pp. 624-629, DOI : 10.14429/dsj.66.9677

Aerodynamic Characterisation of Ramjet Missile through Combined External-internal Computational Fluid Dynamics Simulation

Anand Bhandarkar, Souraseni Basu, P. Manna, and Debasis Chakraborty*

Defence Research and Development Laboratory, Hyderabad - 500 058, India
**E-mail: debasis_cfd@drdl.drdo.in*

ABSTRACT

Combined external-internal flow simulation is required for the estimation of aerodynamic forces and moments of high speed air-breathing vehicle design. A wingless, X-tail configuration with asymmetrically placed rectangular air intake is numerically explored for which experimental data is available for different angles of attack. The asymmetrically placed air intakes and protrusions make the flow field highly three-dimensional and existing empirical relations are inadequate for preliminary design. Three dimensional Navier Stokes equations along with SST-kω turbulence model were solved with a commercial CFD solver to analyse the combined external and internal flow field of the configuration at different angles of attack. Estimated aerodynamic coefficients match well with experimental data and estimated drag coefficient are within 8.5 per cent of experimental data. Intake performance parameters were also evaluated for different angles of attack.

Keyword: Ramjet, computational fluid dynamics, CFD, drag coefficient, pressure recovery, mass capture ratio

1. INTRODUCTION

The superiority of ramjet over solid rocket for improved performance in terms of range, sustained speed, manoeuverability and end game for tactical supersonic missiles is discussed extensively[1-3]. Recently, variable flow ducted rocket engines are proposed and being investigated by many researchers[4-8] due to their long flight range as well as high speed in terminal phase due to its thrust controllability. These fuel rich ducted rocket engines (Fig. 1) use an integral solid propellant rocket to boost the missile to take-over velocity for air-breathing propulsion to perform. In the air-breathing phase of powered flight, fuel - rich effluent from a choked-flow generator mixes and combusts with inlet air in the expended integral booster chamber. This decoupled choked generator flow feature is thus not sensitive to inlet or secondary combustion chamber conditions. This is especially attractive for tactical weapon in high angle-of-attack manoeuvering.

For each flying engine, attainment of good performances results from a satisfactory compromise between drag and thrust. During cruise phase, the missile thrust and drag coefficients are required to be identical. Contrary to a solid rocket motor, the fuel consumption of a variable flow ducted rocket motor engine increases with drag. Higher thrust demand requires a higher fuel to air ratio, while the specific impulse of ram propulsion systems decreases with the reduced air excess at the same time. Hence, the accurate estimation of drag becomes very important. The optimisation of the ram combustor concept is significantly influenced by the demanded average thrust coefficient. While a high thrust demand with a near stoichiometric combustion asks for optimum mixing of the complete air flow with the propellant in the ram combustor dome regime, a low drag configuration with high amount of excess air is best suited for a staged air injection design.

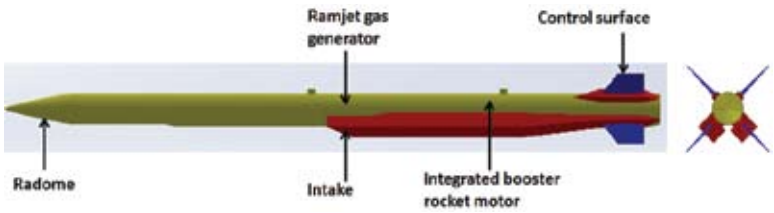

Figure 1. Schematic of variable flow ducted rocket engine.

The forebody shape influences missile drag and air intake distortions. An integrated approach comprising of system drag, forebody volume, seeker demands and air intake performance is required for an optimum overall missile design. The number of air intakes generally results from the mission and consequently from the type of piloting adopted. Positioning of the air intakes is a function of the maximum incidences anticipated.

Supersonic intake for missile has to maintain good performance in velocity change and at manoeuvre, i.e. good characteristics under off-design conditions, such as below and above the designed Mach number with different angles of attack and sideslip. Influence of the distance of the air intakes from the nose of the engine is studied experimentally[9]. Herrmann and Gülhan[10] have shown from the experimental investigation that intake performance differed at different angles of attack ($-30° < \alpha < 30°$) when its axial position is varied along the missile body. Also, due to flow separation, vortex formation, and

Received : 28 January 2016, Revised : 30 June 2016
Accepted : 29 September 2016, Online published : 31 October 2016

varying projected intake cross section and intake compression, intake performance shows a strong dependency on intake roll angle and missile roll angle. Mounting of two intakes (90° apart from each other) on the windward side of the missile was suggested to yield the ideal performance for a ramjet. A downstream intake position close to the combustion chamber is more favourable because of better internal aerodynamics and less weight.

Due to the asymmetric placement of air intakes and other protrusions of high speed air-breathing vehicle, the flow field becomes highly three dimensional and existing empirical relations cannot give useful aerodynamic data for vehicle design. For such a complex flow field, three dimensional CFD becomes a useful tool for the design. Before the numerical tools are used in the design exercise, it is necessary to assess their predictive capabilities to simulate such flow field by taking appropriate validation test cases. Although, separate CFD simulations are carried out for intake[11,12] and combustor[13,14] for variable flow ducted rocket engines, a combined external and internal flow analysis are very rare in the open literature. In fact, the aerodynamic and propulsive elements for any high speed air breathing system are so tightly coupled that proper estimation of aerodynamic characteristics can only be carried out through combined external-internal flow simulations. Saha[15], *et al.* carried out coupled external and internal flow simulation to estimate performance parameters of installed air intakes of a solid fueled integral rocket ramjet at different angles of attack up to 6° and obtained reasonable match with experimental results. Murty[16], *et al.* generated aerodynamic characteristics of a liquid fuel ramjet technology demonstration vehicle through coupled external internal flow analysis and suggested design improvement. Heyes[17] presented important experimental data for aerodynamic characteristics of a series of twin intake air breathing missile configurations with flow through model. Various positions of twin intake configurations, different wing and tail configurations are investigated in details.

In the present work, a flow through model of a twin intake, X-tail configuration of Heyes[17] experimental test is explored numerically to evaluate the predictive capability of commercial CFD software to estimate combined external and internal flow. Three dimemensional Reynolds Averaged Navier Stokes (RANS) equations are solved along with SST-kω turbulence model using Ansys Fluent[18] software. The computed aerodynamic parameters at different angles of attack are compared with experimental results and reasonable match between the computed and experimental results forms the basis of further investigations of external and internal flow patterns through analysis of various flow parameters. Intake performance parameters like mass capture ratio and pressure recovery are evaluated.

2. CONFIGURATION AND TEST DETAILS

Two dimensional cheek mounted twin intake and X-tail configuration (B1I2T2) of Heyes experiment[17] is taken as the test case for validation for the present study and is shown in Fig. 2. Operating conditions and the configuration details are listed in Table 1. The body is an ogive cylinder (L/D =14) and two rectangular intakes are placed with an inlet orientation angle of 135° from the top. The compression ramps of the intakes are 12.5° and 16°, respectively. Capture height and area ratio of the intake duct are 41 mm and 1.24. The intakes are separated from the body through boundary layer diverters located at 43.43 cm from nose tip. Tapered fairing starting from inlet duct end location and extended up to the model base is used. The supersonic tests were conducted in high Mach number test section of Langley Unitary Plan Wind tunnel for Mach no range of 2.5-3.95. The Reynolds number (Re) was maintained constant at 6.56×10^6 per meter.

Table 1. Test conditions and configuration selected[17].

Parameters/configuration	Value
Mach No	2.5
Reynolds No /m	6.56×10^6
AOA	0°, 5°, 7°
Intake	2-D inlet
Intake orientation angle	135° from top
Wing and tail	Wingless, X-tail configuration

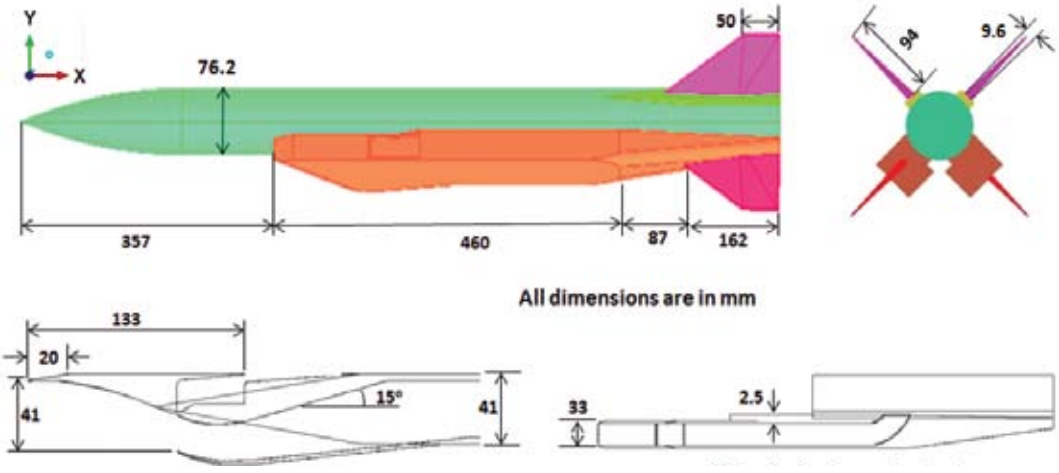

(a) (b)

Figure 2. Model configuration[17] for which the computations are carried out: (a) Intake vertical mid-plane and (b) Intake horizontal mid- plane

3. ANALYSIS

Combined external-internal numerical simulation of aerodynamic model of the ducted rocket configuration (Fig. 2) was carried out by solving three dimensional RANS equations with SST Kω turbulence model using commercial CFD solver Ansys Fluent[18]. Viscosity-affected region (including the viscous sublayer) is resolved with a mesh all the way to the wall. So there is no need for the wall functions. Simulations were carried out at three angles of attack to estimate aerodynamic characteristics and validate the procedure.

3.1 Computational Domain and Grid

Major dimensions of ogive nose cone, cylindrical body, air intake ramp, boundary layer diverter, tapered fairing and X-tail configuration[17] are given in Fig. 2. The computational domain considered for external-internal flow simulation and the schematic of the domain is as shown in Fig. 3 which consists of conical external domain and flow through passage inside the body. The conical domain was selected to capture flow phenomenon accurately at all the angles of attack. The domain inlet starts at 2.6 D ahead of the missile body and is extended up to 22 D, where D is missile diameter (0.0762 m). The domain inlet and exit boundaries are kept 7.87 D and 26 D, respectively. Investigation, no attempt is made to study the wake details of the flow downstream of the body is presented. In a predominant supersonic flow, with limited upstream influence, placement of outflow boundary at 5.4 D downstream of the vehicle base seems adequate. The present configuration is a flow through model for testing aerodynamic performance and internal flow path does not resemble any practical ramjet combustor. In the absence of any internal dimensions of combustor, it was considered as a straight duct. Unstructured grid was generated using ICEM CFD[19]. Two different unstructured grids (coarse one with 2.4 million cells and fine one with 3.6 million cells) were generated to study the grid independence of the results. Grid is very fine near nose, intake and wall regions to capture shocks and viscous affects accurately. The first cell size is of the order of 5 microns. The wall y^+ of ~3 is observed on most of the missile surface. The intake duct inner surface has a y^+ of ~8.The grid distributions over a vertical plane and an intake plane are as shown in Fig. 4.

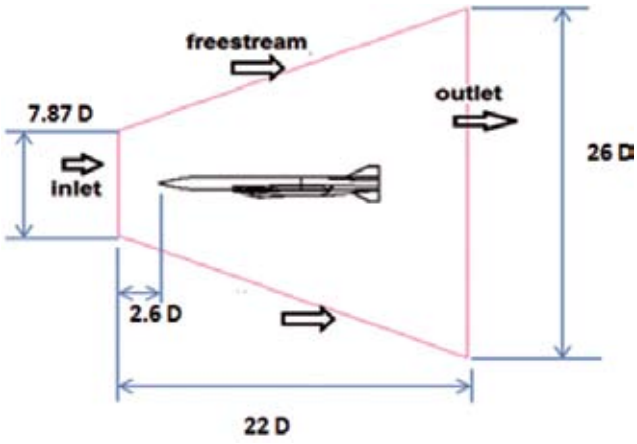

Figure 3. Schematic of computational domain along with boundary conditions.

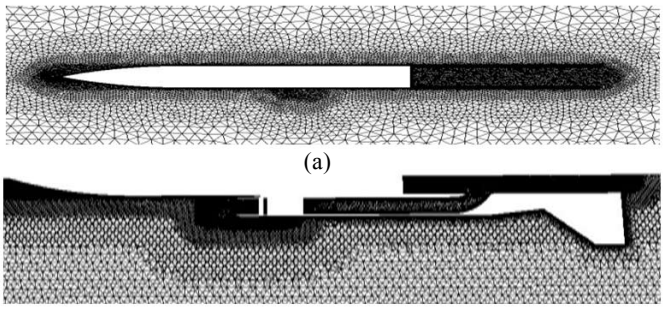

Figure 4. Grid distributions in (a) Vertical plane and (b) Intake plane.

3.2 Boundary Conditions and Numerical Simulations

For the chosen Mach number of 2.5, the test Reynolds no (6.56×10^6 per meter) is matched with the 18.7 km altitude condition and corresponding free stream condition are considered for the simulation. The free stream conditions used in the simulation is presented in Table 2. As the inflow boundary is supersonic, Mach number, static pressure and static temperature were provided at inflow plane. Supersonic outflow boundary condition is prescribed at outlet boundary condition and no slip and adiabatic boundary conditions are provided in the wall. Combined internal-external flow simulation is carried out by using commercial CFD software ANSYS Fluent 14.5[18].

Table 2. Inflow parameters for simulation

Parameters	Value
Mach no	2.5
Static pressure	7003 Pa
Static temperature	205 K

In the numerical simulation, compressible 3-D Navier Stokes equations are solved with SST k-ω turbulence models[20] which blend the attractive features of k- ε turbulence model and k – ω turbulence model. Density based implicit coupled solver is chosen for solving the conservation equations of continuity, momentum and energy simultaneously. Second order accurate Roe's flux difference splitting scheme central differencing scheme are used for spatial discretisation of the inviscid fluxes and diffusion terms respectively. The simulations were carried out for three different angles of attack (α= 0°, 5°, and 7°). To check the effect of altitude, one more simulation for 5° angle of attack was carried out for sea level condition. Force co-efficient like C_D, C_L, C_A, C_N are evaluated from the simulated results and compared with experimental values. The convergence of the simulation is monitored by checking the residue history of mass, momentum and energy and three order fall of maximum residue of mass, momentum and energy were ensured. The achieved mass balance of the simulation is less than 0.001 per cent. Integrated values of C_D and C_L are also monitored over iterations. The C_D and C_L histories for M_∞ =2.5 α= 7° are presented in Fig. 5. It can be observed that after 4000 iterations, both drag and lift coefficients are almost unchanged.

4. RESULTS AND DISCUSSION

Drag co-efficient (C_D) obtained for two different grid size

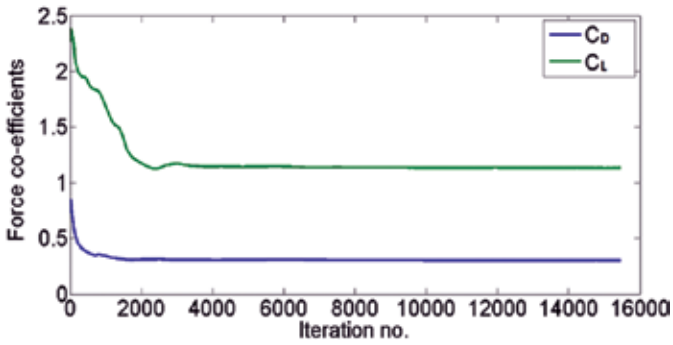

Figure 5. Residue history of drag and lift coefficients.

(2.4 million and 3.6 million) for 5° and 7° angle of attack (α) and 2.5 free stream Mach number are plotted in Fig. 6. Deviation of 4.2-8.5 per cent is observed in drag co-efficient between the computation and experiment[17] as α is changed from 0° to 7°. It is also seen that C_D obtained from two different grid sizes is within 2 per cent demonstrating the grid independence of the results. The qualitative features of the flow field are depicted through Mach number distributions at symmetry plane for three different angles of attacks in Fig. 7. The oblique shocks generated at the tip of the nose cone are clearly visible. The flow features in the windward side of the vehicle body due to the presence of the air intake is crisply captured. The boundary layer thickness at the intake entry plane increases from 2 mm for 0° angle of attack to 2.4 mm at the 7° angle of attack. The cross flow vorticity contours at different axial locations upto the intake plane for 7° angle of attack are shown in Figs. 8(a)

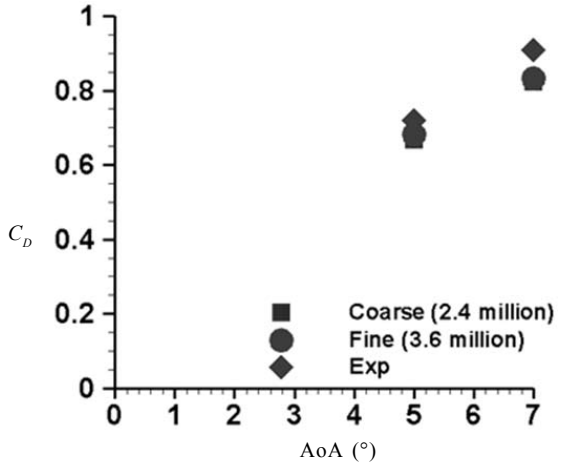

Figure 6. Drag co-efficient for coarse and fine grid.

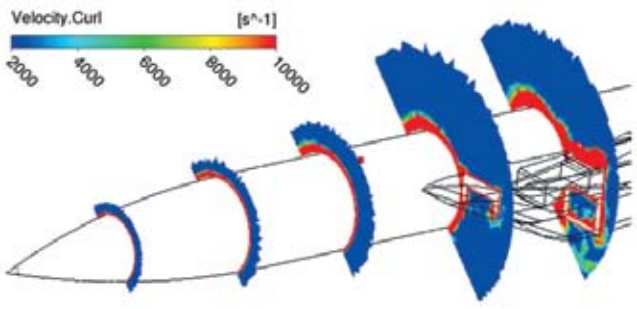

(a)

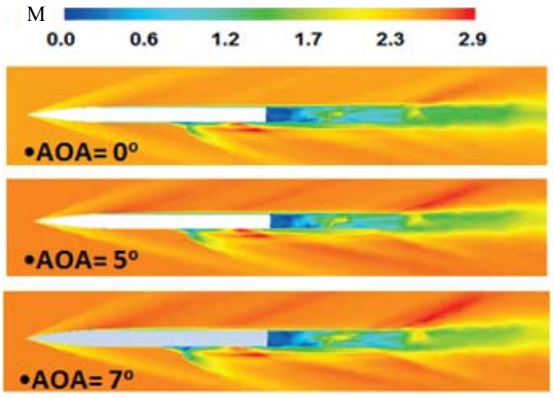

Figure 7. Mach no contour at symmetry plane.

to explain the flow quality at the intake entrance. The growth of the boundary layer along the missile length and flow disturbance at the intake entry is clearly visible in the figure. The vorticity contours in the symmetry plane presented in Fig. 8(b) depict the asymmetry of the flow field in the windward and leeward side of the vehicle surface. Flow is found to decelerate inside the internal flow path as well as in the wake of the body.

Mach number contours at intake plane for different angles of attacks are shown in Fig. 9. With increase in the angle of attack, the oblique shock is seen to move away from the cowl surface which causes spillage of mass flow. The spillage not only reduces the required mass flow rate for proper fuel combustion and also incurs additional spillage drag. Flow deceleration associated with increase in static pressure is visible in the intake region. The amount of spillage increases with the increase in angle of attack. As the angle of attack increases, the shocks emanating from the intake ramps moves upstream, and a detached shock appear in front of the cowl lip. This deflects the incoming flow of air away from the intake entry and reduces the amount of air going into the intake. Due to this spillage increases and the mass capture ratio reduces. However, we did not observe any normal shock ahead of the intake entrance indicating that the intake is not unstarted. Mass capture ratio and pressure recovery coefficients of the intake for different angles of attacks are compiled in Table 3. Mass capture ratio is defined as the ratio of actual mass flow rate through the intake and the maximum possible mass flow through the intake entry plane.

$$\text{Mass capture ratio} = \frac{\dot{m}_2}{\dot{m}_1}$$

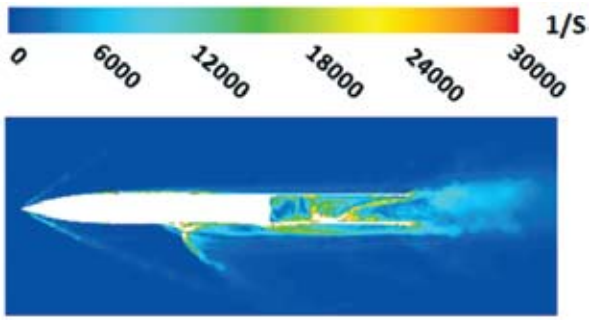

(b)

Figure 8. Vorticity contours at (a) different axial planes and (b) symmetry plane.

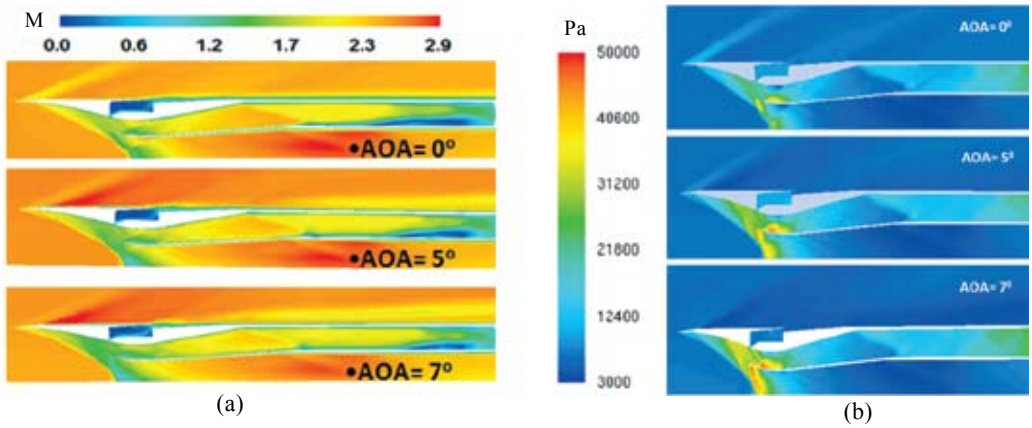

(a) (b)

Figure 9. Mach no contours at intake plane for different angles of attacks (a) external flow path and (b) internal flow path.

The actual mass flow rate is obtained from the simulation by considering a control volume at the intake entrance; while, the maximum possible mass flow rate is calculated based on the frontal area (stream tube area).

$$\dot{m}_1 = A_\infty \rho_\infty V_\infty$$

where A_∞, ρ_∞ and v_∞ are the frontal area, free-stream density and velocity respectively. Pressure recovery is the ratio of total pressure inside intake to the free-stream total pressure.

$$\text{Pressure recovery} = \frac{P_{0\ \text{intake}}}{P_{0_\infty}}$$

Because of the more spillage, mass capture ratio decreases with increase of angle of attack. Mass capture ratio decreases almost 9.8 per cent at α=7° compared to α=0°. Pressure recovery was calculated by comparing total pressure at intake end with free stream total pressure and is given in Table 3. Pressure recovery also decreases with increase in angle of attack.

Table 3. Mass capture ratio and pressure recovery at various angles of attack

Angle of attack	Mass capture ratio	Pressure recovery
0°	0.8108	0.75
5°	0.7455	0.73
7°	0.7314	0.73

The axial force and normal force coefficients were calculated parallel and perpendicular to body axis respectively. The drag and lift coefficients were calculated through force balance parallel and perpendicular to the flow direction, respectively. The comparison of computed aerodynamic coefficients with experimental results[17] for various angles of attack is presented in Figs. 10(a) and (b). Very good overall match is obtained. Computed normal force coefficients (C_N) match extremely well with the experimental data for various angles of attack. The maximum deviation of computation and experimental values for lift coefficient (C_L) and Moment coefficient (Cm) is within 6 per cent. The contributions of pressure drag and viscous drag are presented in Table 4. It was observed that pressure drag component increases with increase in angle of attack while viscous drag remains almost constant. Individual contribution of various parts in drag co-efficient estimation is examined and the results are presented in Table 5. It was observed that vehicle body, outer part of intake and tail fins contribute higher drag force (~93 per cent) while missile base, boundary layer diverter and tail fairings together contribute less than 6.3 per cent. With the increase of angle of attack, drag co-efficient increases for all the components.

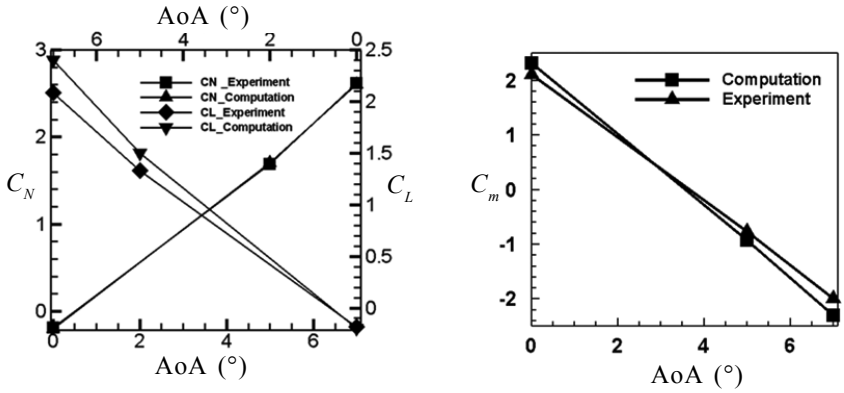

Figure 10. Comparison between experiment and computation (a) Normal force coefficient and Lift coefficient and (b) Moment coefficient.

Table 4. Contribution of pressure and viscous drag

M_∞	α (in deg)	Pressure drag (% of total drag)	Viscous drag (% of total drag)	Total drag
2.5	0	0.329 (60)	0.217 (40)	0.546
2.5	5	0.462 (68)	0.22 (32)	0.682
2.5	7	0.61 (73)	0.223 (27)	0.833

Table 5. Drag coefficient of various component

Parts	C_D α = 0°	% of total drag	C_D α = 5°	% of total drag	C_D α = 7°	% of total drag
Vehicle body	0.1826	33.5	0.2482	36.4	0.3054	36.7
Vehicle base	0.0105	1.9	0.0113	1.7	0.0115	1.4
Diverter	0.0099	1.8	0.0171	2.5	0.0189	2.3
Intake outer part	0.2098	38.4	0.2358	34.6	0.2828	33.9
Tail fairing	0.0186	3.4	0.0187	2.7	0.0218	2.6
Tail fins	0.1148	21	0.1504	22.1	0.1922	23.1

5. CONCLUSION

Numerical simulation of a combined external-internal flow path of a twin intake X-tail configuration is carried out. 3D RANS equations along with SST-kω turbulence model is solved using commercial CFD solver. Grid independence of the solutions is demonstrated and various flow parameters are captured crisply in the simulations. Computed normal force co-efficient has shown very good match (~0.5 per cent) with measurements. Computed drag coefficients at different angles of attack compare well (4.2 - 8.5 per cent) with experimental data. Pressure drag component increases with increase in angle of attack while viscous drag remains almost constant. Missile body, intake outer part and tail fins together contribute more than 90 per cent of the total drag; while the contribution of other components are very less. The spillage through the intake increases with increase in angle of attack which eventually increases the intake drag.

REFERENCES

1. Waltrup, P.J.; White, M.E.; Zarlingo, F. & Gravlin, E.S. History of U.S. navy ramjet, scramjet, and mixed-cycle propulsion development. *J. Propulsion Power*, 2002, **18**(1), 14-27. doi: 10.2514/2.5928
2. Fry, R.S. A century of ramjet propulsion technology evolution. *J. Propulsion Power*, 2004, **20**(1), 27-58. doi: 10.2514/1.9178
3. Calzone R.F. Developments in missile ramjet propulsion. Report No. TNO report. PML 1996-A100, 1996.
4. Besser H L, Hermann L. W**.** The ducted rocket propulsion system for meteor and its background in German airbreathing motor technology. Paper No. ISABE-2005-1149
5. Besser, H.L.; Hermann, L.W. & Kurth, G. Fit for mission-design tailoring aspects of throttleable ducted rocket propulsion systems. AIAA -2008- 5262. doi: 10.2514/6.2008-5262
6. Moerel J. L.P.A, Calzone R.F, Halswijk W.H.C, Horst R.M. V, Stowed R and Lauzontt M. Performance simulations of a rocket- and a ramjet air-to-air missile. AIAA-2001-4412. doi: 10.2514/6.2001-4412
7. Besser, H.L. History of ducted rocket development at bayern-chemie. AIAA 2008-5261. doi: 10.2514/6.2008-5261
8. Yoshihiro, Y.; Yoshiyuki, I.; Hisahiro, N.; Eishu, K.; Junichi, S.; Yuichi, O. & Akihiko, Y. Performance demonstration of a variable flow ducted rocket engine by test flight. AIAA 2009-5031. doi: 10.2514/6.2009-5031
9. Laruelle, G. Air intakes for a probative missile of rocket ramjet. NASA TM-77407, 1984.
10. Herrmann, D. & Gülhan, A. Influence of intake orientation on ramjet performance. *J. Propulsion Power*, 2010, **26**(4), 848-857. doi: 10.2514/1.47140
11. Moerel, J.L.; Veraar, R.G.; Halswijk, W.H.C.; Pimentel, R.; Corriveau, D.; Hamel, N.; Lesage, F. & Vos, J.B. Internal flow characteristics of a rectangular ramjet air intake. AIAA Paper 2009-5076**.** doi: 10.2514/6.2009-5076
12. Hidenori, T.; Kenji, K.; Yoshiyuki, I.; Junichi, S. & Akihiko, Y. Development of wide-range supersonic intake for variable flow ducted rocket engine. AIAA Paper 2009-5223. doi: 10.2514/6.2009-5223
13. Stowe, R.A.; Champlain, A.D. & Mayer, A.E.H.J. Modelling combustor performance of a ducted rocket. AIAA Paper 2000-3728. doi: 10.2514/6.2001-3193
14. Ristori, A. & Dufour, E. Numerical simulation of ducted rocket motor. AIAA Paper 2001-3193. doi: 10.2514/6.2001-3193
15. Saha, S.; Sinha, P.K. & Chakraborty, D. CFD prediction of ramjet intake characteristics at angle of attack. *J. Aerospace Sci. Technol*., 2010, **62**(3), 159–165.
16. Murty, Chandra M.S.R. & Chakraborty D. Coupled external and internal flow simulation of a liquid fuelled ramjet vehicle. *J. Aerospace Sci. Technol.,* 2014, **36,** 1–4. doi: 10.1016/j.ast.2014.03.011
17. Hayes, C. Aerodynamic characteristics of a series of twin-Inlet airbreathing missile configurations. NASA Technical Memorandum 84559, Langley Research Center, Virginia, 1983.
18. Fluent12.1, Theory manual, Ansys Inc, 2009.
19. ICEMCFD, 11.0 Modeling, Meshing Guide, Ansys Inc. 2007.
20. Menter, F.R. Two-equation eddy-viscosity turbulence models for engineering applications. *AIAA-Journal,* 1994, **32**(8), 1598-1605. doi: 10.2514/3.12149

CONTRIBUTORS

Mr Anand Bhandarkar obtained his MTech in Mechanical Engineering from IIT, BHU. Presently he is working as a Scientist at the Defence Research and Development Laboratory (DRDL), Hyderabad. His research areas include : Aerodynamic heating, droplet break-up study for high-speed flow, two phase flow analysis, CHT analsys, Base flow analysis. In current study, he has carried out grid generation, numerical simulation and analysis of the results.

Ms Souraseni Basu did her BE (Hons.) in Chemical Engineering and ME in Aerospace Engineering from NIT, Durgapur and IISc, Bangalore, respectively. She worked extensively in Rocket and Ramjet Propulsion and process scale up of High Energy Materials in DRDL and HEMRL. Currently she is working DOCD, DRDL and working on analysis of reacting flow for high speed applications. She has participated in problem formulation, grid generation, simulation, post processing of results and preparation of manuscript.

Dr P. Manna obtained his PhD (Thermal Science and Engineering) from IIT, Kharagpur. Presently he is working as a Scientist in the Directorate of Computational Dynamics, DRDL, Hyderabad. His research interests include: CFD, propulsion, heat transfer, and high-speed reacting flow. In current study, he has participated in numerical simulation, analysis of the results and preparation of the paper.

Dr Debasis Chakraborty did his PhD in Aerospace Engineering from IISc, Bangalore. He has worked in VSSC (ISRO) and DRDL(DRDO) for last 29 years. Currently, he is Technology Director, computational dynamics and guiding the numerical simulations for both aerodynamics and propulsive characterisation of different missiles. He has contributed in problem selection, guidance and preparation of manuscript.